https://doi.org/10.2352/EI.2023.35.15.COLOR-204

Impact of a coating layer on the appearance of various halftone patterns

Fanny Dailliez [1,2], Mathieu Hébert [2], Lionel Simonot [3], Lionel Chagas [1], Thierry Fournel [2], Vincent Duveiller [2], Anne Blayo [1]
[1]Univ. Grenoble Alpes, CNRS, Grenoble INP (Institute of Engineering Univ. Grenoble Alpes), LGP2, 38000 Grenoble, France;
[2]Université Jean Monnet Saint-Etienne, CNRS, Institut d Optique Graduate School, Laboratoire Hubert Curien UMR 5516, F-42023, SAINT-ETIENNE, France ; [3] Université de Poitiers, Institut Pprime UPR CNRS 3346; Futuroscope Chasseneuil, France.

Abstract

Coating a printed surface with a smooth transparent layer can modify its color. This is due to light interreflections within the coating layer which produce a halo-shaped point spread function. The change of color is related to the coating thickness and the halftone screening used for printing. Thanks to an optical model able to predict the spectral reflectance of the coated print from the one of the non-coated print, we propose to study the impact of the halftone pattern (shape and profile) on the color change caused by the coating layer. It was found that line halftone patterns with a crenel profile induces the strongest changes of color. This is therefore the pattern that we use for an innovative application of this phenomenon: revealing a binary image by adding or removing a coating layer on the print that is originally uniform.

Introduction

Since the 1930s, the appearance of prints has been studied to improve color management during the printing process. The early optical models derive the color appearance of a print from the reflectance of the inked dots printed on the substrate, their area, and the reflectance of the substrate [1–3]. As the printing processes have been improved, inked dots have become smaller, indistinguishable by the naked eye at a reading distance. Optical models progressively adapted to an optical phenomenon which had been previously overlooked: the effect of light diffusion within the substrate [4–6]. This phenomenon, called *optical dot gain*, enables light to transit from non-inked areas to inked areas (and vice versa), which tends to blur the borders of the inked areas and to darken the colors of the halftone print, due to an increased absorbance by the ink dots. This effect can be modelled by convolutions between the spatial and spectral transmittance of the inked dots and the point spread function (PSF) of this light diffusion [7–9]. In the literature, this PSF is often considered to be gaussian-shaped [10–13]. It has been shown recently that coating a smooth transparent layer (varnish, lamination) over a print tends to induce an additional dot gain which decreases its reflectance and induces a darkening of the color well visible in figure 1 A). This phenomenon, that we called "halo effect", is caused by light propagation inside the transparent layer [14]. It has a very specific halo-shaped PSF, displayed in figure 1 B), caused by the internal reflections of light by the coating-air interface [15], [16]. This phenomenon has been mainly studied in case of halftones composed of inked lines, and it has been shown that there is a ratio between the coating thickness and the halftone period for which the decrease of reflectance reaches a maximum [17]. A first objective of this study is to find the 2D halftone pattern which maximises the darkening caused by the addition of a coating layer. A second objective is to estimate the impact of the optical dot gain due to light scattering within the substrate in the darkening induced by the halo effect. Both objectives were studied through simulations presented in Section 1. From the simulations, an application has been developed that is presented in Section 2.

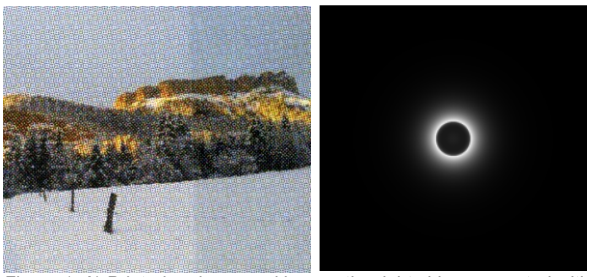

Figure 1. A) Printed and scanned image, the right side was coated with a tape layer. B) Halo shaped PSF induced by the internal reflection inside a smooth transparent layer in optical contact with a Lambertian surface.

1. Simulations of the halo effect on various patterns

The method used to simulate the halo effect is presented in a first subsection. The simulation results obtained with this method are detailed in two subsections evaluating respectively the influence of the shape of 2D halftone patterns on the darkening due to the halo effect, and the influence of the dot gain due to light scattering within the substrate, impacting the halftone profiles, on the darkening effect.

Simulation method

A print is composed of inked and non-inked areas whose distribution is described by a halftone screen. Its spectral reflectance factor varies spatially according to this spatial distribution**.** If the print is not coated, its global spectral reflectance factor is equal to the arithmetic spatial average of the spectral reflectance factor. If the print is coated with a very thick layer with respect to the size of the reflectance distribution, its global spectral reflectance factor can be modelled with the Williams-Clapper model [18], [19]:

$$R(\lambda) = r_s + \frac{T_{in}T_{out}\overline{\rho}(\lambda)}{1 - r_i\overline{\rho}(\lambda)}$$

where $\overline{\rho}$ is the spatial average of the intrinsic spectral reflectance of the print at wavelength λ, and r_s, r_i, T_{in}, and T_{out} are the fractions of light reflected and transmitted by the interface between the coating and air. The latter four parameters are displayed in figure 2. r_s is the fraction of light externally reflected by the air-coating interface, r_i the one internally reflected inside the layer, T_{in} the fraction of light transmitted by the interface towards the coating and T_{out} the one transmitted towards the sensor. Considering that the coating has the same optical index as the printing support (n_1 = 1.5), these parameters remain the same whether the print is coated or not. They depend on the measurement geometry and on the Fresnel reflectance and transmittance at the interface [20].

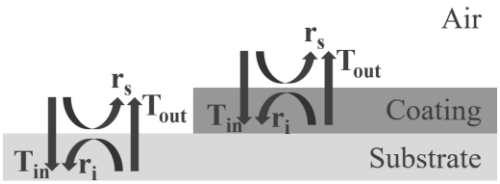

Figure 2. Light transfers at the interface with air.

The measurement geometry selected for the simulations has been introduced in a previous study experimentally verifying the optical model related to the halo effect through spectral microscopic measurements [14]. In this study the instrument had a 0°:0° geometry with the specular reflection excluded with polarizers in a crossed configuration. For this geometry, and considering an interface between a medium of optical index n_1 = 1.5 and air of optical index n_0 = 1,

$r_s = 0$,

$T_{out} = \frac{1-R_{n_0 n_1}(0°)}{\pi {n_1}^2} = \frac{0.427}{\pi}$,

$r_i = \int_0^{\frac{\pi}{2}} R_{n_1 n_0}(\theta) \sin(2\theta)\, d\theta = 0.596$

$T_{in} = 1 - R_{n_0 n_1}(0°) = 0.960.$

where $R_{n_1 n_0}$, respectively $R_{n_0 n_1}$, denote the Fresnel reflectance at the interface between the printed materials and air when light comes from the print, respectively from air. The factor $1/\pi$ in T_{out} cancels when the radiance measured from the sample is divided by the radiance $1/\pi$ measured from a perfect white diffuser (illuminated with an irradiance unity) in order to obtain the reflectance factor *R*. The objective of the simulations presented in this paper is to evaluate the darkening effect of coating layers of intermediate thicknesses with respect to the size of the halftone reflectance distributions. The aim is thus to link the two limits between a non-coated halftone reflectance, and the one described by the Williams-Clapper model for large coating thicknesses, and potentially find the halftone pattern minimizing the reflectance factor. The simulations rely on an optical model which describes the multiple interreflections of light inside the coating layer. Light reaching and being reflected by the printed substrate can be trapped within the coating layer due to the difference of optical index between the coating layer and air. The light rays reaching the coating-air interface with an angle of incidence higher than the critical angle $\theta = \arcsin(n_0/n_1)$ are completely reflected within the coating, inducing the halo PSF presented in figure 1 B). Finally, the spectral reflectance factor, *R*, of the coated halftone at a point (*x, y*) and at a given wavelength is:

$$R(x,y) = r_s + T_{out} \sum_{k=1}^{10} M_k(x,y) \qquad (1)$$

Function M_k describes the exitance of the substrate after the k^{th} reflection of light inside the coating layer — the exitances after the 10th reflection are close to zero, the sum is then truncated —:

$$M_k(x,y) = \rho(x,y)[M_{k-1} * h](x,y) \qquad (2)$$

where $\rho(x,y)$ is the spatial intrinsic reflectance of the printed support at the considered wavelength, which can be derived from the reflectance factor $R_{NC}(x,y)$ of the non-coated halftone through the Williams-Clapper model:

$$\rho(x,y) = \frac{R_{NC}(x,y) - r_s}{T_{in}T_{out} + r_i[R_{NC}(x,y) - r_s]} \qquad (3)$$

In equation (2), spatial function *h* describes the halo PSF:

$$h(x,y) = \frac{4d^2 R_{n_1,n_0}\left(arctan\left[\frac{\sqrt{x^2+y^2}}{(2d)}\right]\right)}{\pi(x^2+y^2+4d^2)^2} \qquad (4)$$

where R_{n_1,n_0} is again the Fresnel reflectance at the coating-air interface, and *d* is the thickness of the coating layer.

The first exitance in equation (2) depends on the irradiance *E* of the printed support:

$$M_1(x,y) = T_{in}\rho(\mathrm{x,y})E \qquad (5)$$

As can be seen in equation (2), interreflections inside the coating layer depend on the PSF *h* thus on the thickness of the coating layer *d*, and on the spatial intrinsic reflectance of the halftone, *ρ*. If the halftone is periodic, with a period *p*, the darkening caused by the coating layer depends only on the spatial and spectral reflectance factor of the halftone pattern and on the ratio *d/p*. The first simulations aimed at observing the darkening effect on various binary 2D patterns.

Influence of 2D halftone patterns

To evaluate the influence of the halftone pattern on the darkening effect, simulations were performed with various monochrome binary halftone screens. The reflectance factors were described on two-dimensional cells of dimension $p \times p$ pixels. Each cell was repeated along the *x* and *y* axis to generate a halftone screen whose area is large enough to prevent edge issues during the multiple convolution process. The halftone screen thus generated had a surface coverage of 0.5, and the reflectance factors of the non-coated print were arbitrarily set to 0.1 for the inked areas and 0.9 for the non-inked areas, for all wavelengths. These reflectance factor values were chosen to prevent total absorption of the light reaching the inked areas and have a global reflectance factor without coating of 0.5. Various shapes were selected, presented in figure 3, among which a line pattern, a chess pattern, a "circle" pattern of shape quite similar to the halo PSF, and a random pattern of rather high spatial frequency.

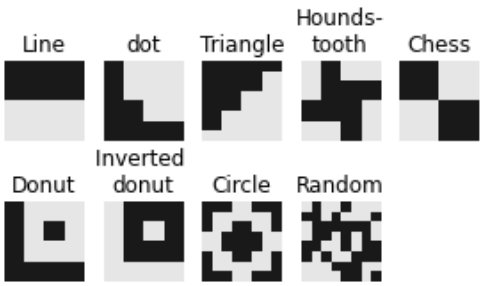

Figure 3. Simulated halftone patterns, dark areas have a reflectance of 0.1 and clear areas have a reflectance of 0.9, (p = 8).

The simulated global reflectance factors of the various halftone shapes presented in figure 3**,** predicted with the multi-convolutive model presented in equations (1) – (5), are displayed in figure 4 as a function of *d/p*.

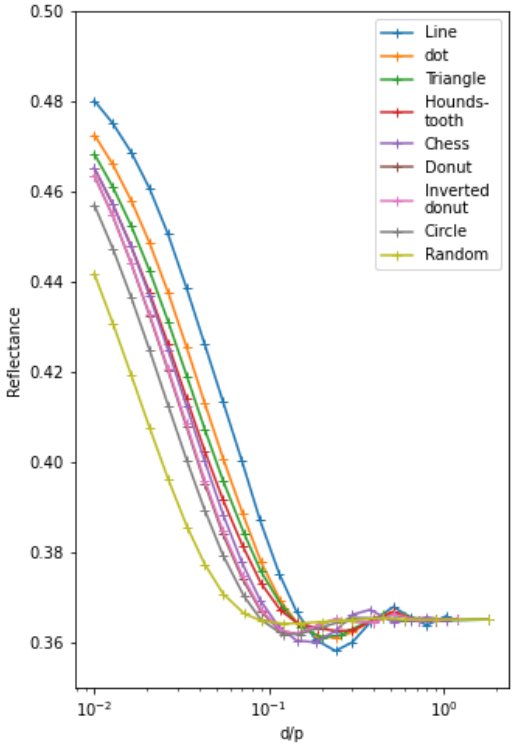

Figure 4. Average reflectance factor of various halftone patterns as a function of the ratio between the thickness of the coating layer, d, and the period of the halftone screen, p.

As expected, when the coating thickness tends to 0, i.e., $d/p \rightarrow 0$, the average reflectance factor gets closer to the bound of 0.5 for all patterns. Similarly, when $d/p \rightarrow +\infty$, the pattern period is so small with respect to the coating thickness that the halftone can be considered uniform and the halftone reflectance factors also reach the limit of 0.37 defined by the Williams-Clapper model [18].
The results show that for $d/p < 0.1$, at a given d/p, patterns composed of small, dispersed dots are more darkened by the coating layer than patterns with few dot-dispersion. This is because light meeting patterns composed of small, dispersed dots can easily travel from one inked area to another one. For a small d/p, the overall halftone dot shape matters then less than the spatial frequency or perimeter of the small dots within it, this is particularly depicted by the fact that the curves of the donut and inverted donut are almost superimposed.
Yet, the pattern presenting the overall strongest darkening is the line pattern. Indeed, for $d/p \approx 0.2$, it reaches a minimum below the reflectance factor limit given by the Williams-Clapper model which is due to the multiple convolutions between the halo shaped PSF and the line shapes.

In the simulations presented in figures 3 and 4, the halftone screens have a binary reflectance distribution between inked and non-inked areas. In practice, light diffusion within the substrate can smoothen the spatial reflectance at the borders between inked and non-inked areas, making the intrinsic reflectance of the halftone, $\rho(x, y)$, vary continuously along the halftone profile. The second simulation was then designed to evaluate the impact of a coating layer on various halftone profiles, thus simulating various dot gains due to light scattering within the substrate.

Influence of halftone profiles

To simplify the problem, unidimensional line halftones have been selected, with different reflectance factor profiles displayed in figure 5. The first profile is a step, which would be observed with perfectly printed halftones not subject to dot gain, and the second profile is a sinusoidal one, which is a rough approximation of the profile observed on prints strongly impacted by the optical dot gain due to light scattering within the substrate. For comparison purposes, a triangular profile has also been considered in the simulations. The triangular profile ranges between the lowest reflectance factor value 0.1 and the highest value 0.9, as for the patterns shown in Figure 3. In the sinusoidal pattern, the reflectance factor ranges between 0.17 and 0.83, and in the step pattern, it is 0.27 and 0.74. These minimum and maximum values are defined in order to have the same limit of the global reflectance factor R as d/p tends to infinity (therefore the same spatial average of the intrinsic reflectance ρ, set to 0.67) and the same limit of R as d/p tends to zero.

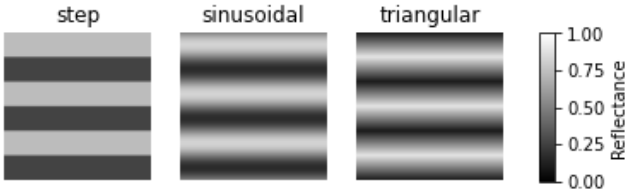

Figure 5. Simulated line profiles, step, sinusoidal, and triangular, of respective reflectance range [0.27; 0.74], [0.17; 0.83], and [0.10; 0.90].

The results for the different halftone profiles presented in figure 5 are displayed in figures 6 & 7.

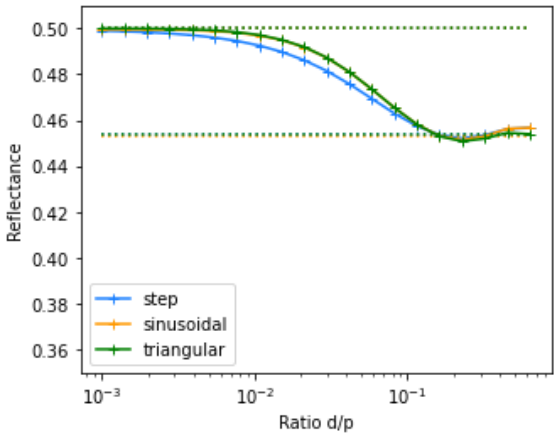

Figure 6. Average reflectance of the line halftone of various profiles as a function of d/p.

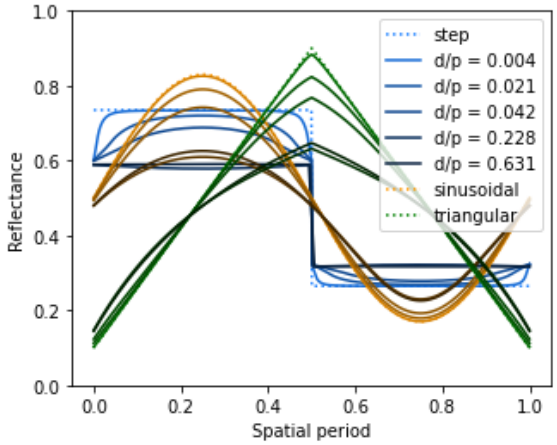

Figure 7. Spatial reflectance profile of line halftones over one period for various d/p.

These graphs enable to see the darkening effect caused by the coating layer, both on the global reflectance factor and on the spatial reflectance factor of the print. It can be observed that the step profile is more impacted by the coating layer than the other profiles: it intervenes for smaller *d/p* than for the triangular or sinusoidal profiles, figure 6. The sharp edges of the step profile smoothen significantly as light propagates farther within the coating layer, whereas the impact on the sinusoidal profile is mainly on the amplitude of the reflectance factor, figure 7. The darkening of the clear areas is slightly compensated by an increase of reflectance of the dark areas as the coating enables light to propagate from inked areas to non-inked areas as well as the other way around. There is still yet a global darkening of the prints as light has more probability to reach an absorbing area when the print is coated than when it is not.

To conclude, these simulations showed that both the halftone shape and profile have an impact on the darkening caused by the addition of a coating layer. Line halftones can be the most impacted by the coating layer, and, at a given coating thickness, the color change is happening at a smaller period than the other shapes. It can also be concluded that a print subject to a lot of dot gain within its substrate will be less impacted by a coating layer than the prints less subject to dot gain having a sharp profile, see figure 7.

These simulations were performed on achromatic simulated prints but can be applied to colored prints by considering the spatial reflectance independently at each wavelength. To apply the multi-convolutive model, one needs to evaluate the spatial and spectral reflectance of a print, which can be done from measurements of a multispectral microscope [14], another method, fully numerical, would be to apply optical models to the nominal print to generate a simulated non-coated print [11].

2. Application: hidden images

The previous section showed that the halftone pattern and the dot gain due to scattering within the substrate can have a strong impact on the darkening effect caused by the addition of a coating layer. The objective in this section is to use the dot gain from the substrate and the halo effects to find two halftones, one for the image and one for the background, such that under one coating layer they appear the same, whereas by adding or removing a coating layer, they appear differently, revealing a hidden image.

Hidden image designs

To generate such a hidden image, one of the halftones shall be only slightly impacted by the darkening caused by the halo effect whereas the other one shall be significantly impacted. We then chose two halftones consisting of line patterns with different periods. The periods were comprised between two limits: the smallest printable period is limited by the resolution of the printer, and the largest period is limited by the eye perception: if the periods are too large, the pattern lines become perceptible by the naked eye. One pattern had a small period p_1 = 0.180 mm, strongly impacted by the optical dot gain within its substrate, and the other one had a larger period p_2 = 0.479 mm. With a coating of thickness $d = 24$ µm, the thin pattern has a ratio $d/p_1 = 1.3 \cdot 10^{-1}$, and the large one: $d/p_2 = 5.0 \cdot 10^{-2}$. For these ratios, the reflectance factor of the large period halftone varies significantly by adding a second coating layer ($2d/p_2 = 1.0 \cdot 10^{-1}$) whereas the reflectance factor of the small period halftones varies only slightly by addition of a coating layer ($2d/p_1 = 2.6 \cdot 10^{-1}$), see figure 8 where the line profile is extracted from figure 4. Furthermore, the large pattern is less impacted by optical dot gain than the thinner one, which could amplify the difference of darkening, as shown in figures 6 & 7. It can be also noted that the shape of the small period pattern does not really matter as long as the period is small enough for the reflectance factor to be relatively unaffected by addition of coating layers.

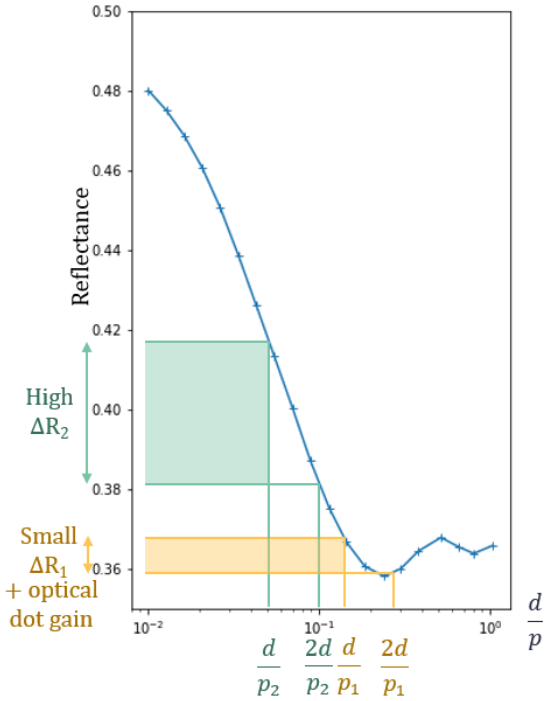

Figure 8. Simulation of the reflectance factor differences, ΔR_1 and ΔR_2, respectively of the thin line halftone and the large line halftone, which would be obtained by addition of a coating layer if the printed patterns were identical to the line pattern simulated in figure 4.

Based on the observations above, the thin pattern was designed with a 6 × 6-pixel threshold matrix displayed in figure 9 A). The large pattern was designed with a 16 × 16-pixel threshold matrix displayed in figure 9 B). The lines were inclined by a 45° angle to be less detectable by the naked eye than horizontal or vertical lines.

The printer was a Xerox Versant 180, printing at 600 dpi. The substrate was a white bright paper. The coater was the laminator DRY 350 from RBS, coating a smooth transparent foil composed of OPP of thickness approximately equal to 24 µm.

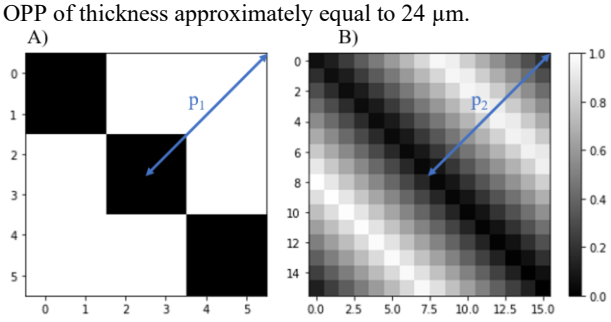

Figure 9. A) Threshold matrix of the thin pattern; B) threshold matrix of the large pattern. For a given halftone surface coverage, all the pixels of the threshold matrix having a grey value inferior to this surface coverage are inked.

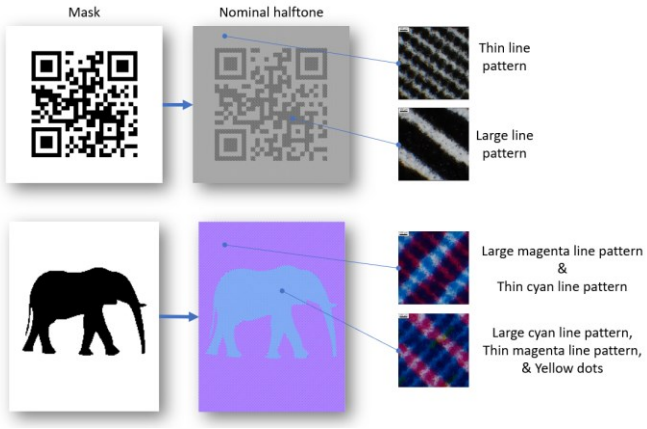

Figure 10. Top: design of the test form composed of black lines with a QR-code mask, bottom: design of the test form mainly composed of cyan and magenta lines, with an elephant mask.

The nominal surface coverage of the thin pattern was arbitrarily set to 33.3%, which results in an effective surface coverage around 50% due to mechanical and optical dot gain within the substrate. As the thin pattern is more subject to mechanical and optical dot gain within the substrate than the large pattern, the nominal surface coverage of the larger halftone shall be higher for the two halftones to have the same appearance. The surface coverage of the larger halftone was evaluated experimentally through spectral measurements of lookup tables of prints with one coating layer. The spectral measurements were performed with the spectrophotometer CM 2600d from Konica Minolta (di:8°, 8 mm aperture, UV included). The selected surface coverages of the large lines were the ones minimizing the color difference ΔE_{00} under D65 illuminant between the image and the background coated with one layer.

Two test forms were designed on this basis: one composed of black lines printed on a white paper with a QR-code image, presented in top position in figure 10, the other one mainly composed of superimposed cyan and magenta lines of different periods with an elephant image, displayed at the bottom position in figure 10. To better adjust the appearance match of the two halftones areas (image and background) of this last test form, yellow dots were added to the image area. Cyan and magenta lines had different orientations to prevent Moiré effects. The nominal surface coverage of the large black lines was found to be 54%, the one of the large magenta lines was 52%, the one of the large cyan lines was 53%, and the one of the yellow dots was 3%.

Hidden images

Three identical test forms were printed for each image: one was not coated, the second was coated with one layer, and the third was coated with two layers. The surface coverages of the different areas of the test forms were adjusted to have a color match with one coating layer.

The visible color changes for different coatings used for the image hiding can be characterized with macroscale spectrophotometric reflectance factor measurements. The reflectance factor around the blue disks in figure 10 was measured on each test form with the spectrophotometer i7 from X-Rite (di:8°, 6 mm measurement aperture, 17 mm illumination aperture, UV excluded, average on 7 consecutive measurements). The differences of reflectance factor between the background and the image are displayed in figure 11 for each coating layer.

In this figure, a negative reflectance factor difference implies that the background has a smaller reflectance than the image, thus that it appears darker than the image. In the QR-code picture, the background is darker than the image when the print is non-coated, they have a similar reflectance factor when the print is coated with one layer (the reflectance factor difference is near 0), and the image is darker than the background when the print is laminated two times. This is due to the fact that the large lines composing the image are more impacted by the darkening caused by the halo effect than the thin lines composing the background. In terms of color difference between the QR-code image and its background estimated with ΔE_{00} under D65 illuminant [21], there is a difference of ΔE_{00} = 1.38 without coating, ΔE_{00} = 0.99 with one coating layer, and ΔE_{00} = 1.25 with two coating layers. The image can then be rather successfully hidden with one coating layer and revealed by adding or removing a coating layer.

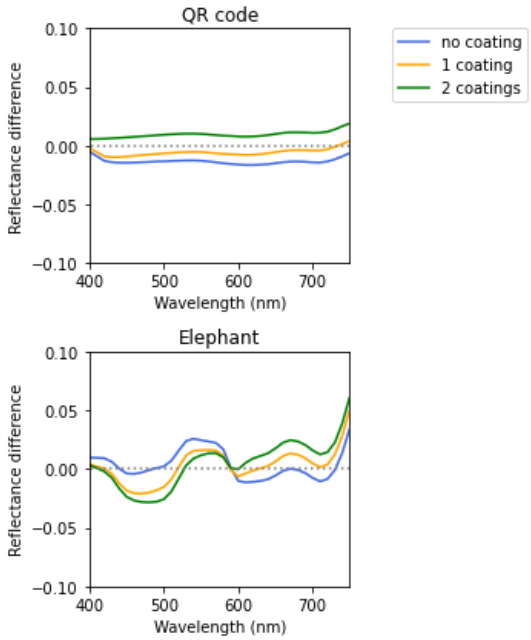

Figure 11. Difference of reflectance measurements between the background and the image for each coating layer. Top: black and white QR-code picture; bottom: color elephant picture.

For the color elephant test form, the color matching with one coating layer was more difficult to obtain. The difference of reflectance factors between the background and the image is farther to zero than the one of the QR code. Metamerism between the elephant and the background was observed both for the non-coated test form and on the one coated with one layer, depending on the illumination. As the elephant image is composed of large cyan lines, its reflectance factor at long wavelengths tends to decrease by addition of coating layers. Similarly, the background, composed of large magenta lines, absorbs more light in the short wavelengths as the coating thickness increases. As a result, the reflectance factor difference shown in figure 11 decreases by addition of coating layers at the short wavelengths and increases at the long wavelengths. The color difference between the elephant image and the background under D65 illuminant is $\Delta E_{00} = 3.02$ without coating, $\Delta E_{00} = 1.73$ with one coating layer, and $\Delta E_{00} = 2.32$ with two coating layers.

The generated hue shifts are visible in the pictures displayed in figure 12. It can be noticed that the pictures do not perfectly reflect the visual appearance of the prints, especially as the printed lines tend to interfere with the anti-aliasing filter of the camera. The middle pictures appear less contrasted than the others, the image hiding is then rather successful for the pictures with one coating layer. For the QR-code picture, the images appear lighter than the background on the image without coating, and darker than the background with two coating layers. The image is then rather well revealed by addition or removal of a coating layer. For the elephant pictures, the elephant image shifts from pinkish on a bluish background for the test form without coating, to a blue elephant on a pinker background with two coating layers, revealing also the image hidden under one coating layer.

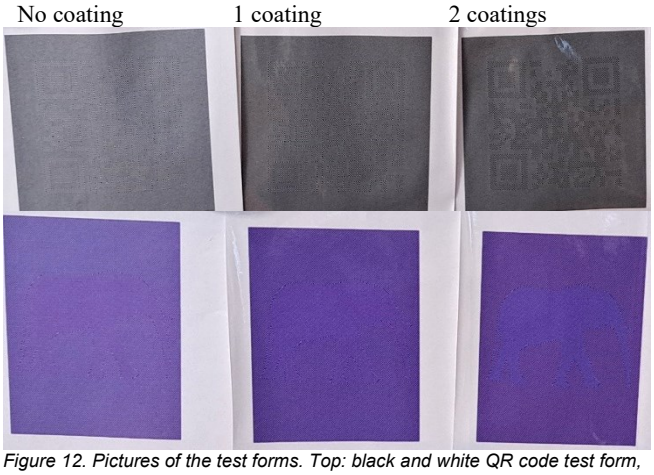

Figure 12. Pictures of the test forms. Top: black and white QR code test form, bottom: color elephant test form. Left: no coating layer, middle: one coating layer, right: two coating layers. The surface coverages were adjusted to have a color match between the image and the background with one coating layer.

Lastly, it was observed that the hidden image could also be revealed by illuminating the test forms from the backside (in transmission mode) as displayed in figure 13. With this illumination mode, light rays transit in the substrate before being possibly absorbed by ink or reaching the eye. This significantly reduces optical dot gain within the print due to light diffusion inside the substrate. In reflection mode, thin lines were more impacted by optical dot gain from the substrate than large lines as thin lines have a longer perimeter. Thus, in transmission mode, thin lines appear significantly lighter, revealing the hidden image. The effect is even more pronounced when the printed is coated due to the halo effect.

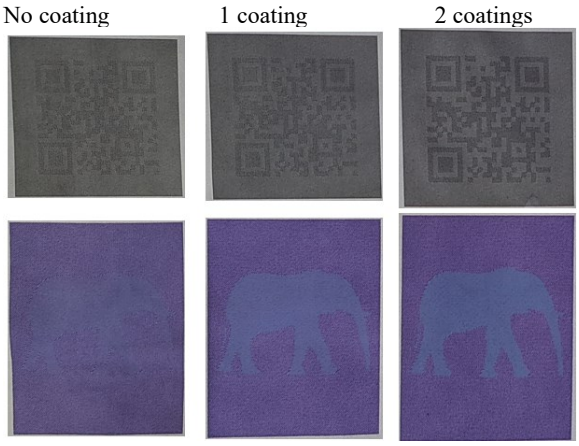

Figure 13. Pictures of the test forms in transmission mode.

Conclusion

Adding a coating layer over a print decreases its reflectance, which can be predicted with a multi-convolutive model already tested experimentally. In this paper, the model is used to evaluate the influence on the darkening effect of the halftone shape and profile. In general, for a given coating thickness and halftone period, halftone screens composed of small patterns yield a stronger darkening than the ones composed of large patterns. Regarding the

pattern shape, the line pattern is the one which reaches the overall minimal reflectance, for a specific *d/p ratio* between the coating thickness *d* and the halftone period *p*, due to the multiple convolutions between the line pattern and the ring-shaped PSF linked with the coating. It was also shown that for a given *d/p* value, halftones with sharp profiles darken more than halftones with a smoother profile, especially when the profiles have the same reflectance range. Thus, the reflectances of halftones subject to optical dot gain due to light scattering within the substrate are less impacted by the addition of a coating layer than halftones which are not impacted by dot gain.

These observations on the influence of the halftone shape and profiles on the darkening caused by the coating layer enabled to design pictures containing a hidden image. The image was hidden when coated with one lamination layer and could be revealed by adding or removing a coating layer, or by observing the picture in transmission mode. To hide this image, two halftones screens were designed, one for the image and one for the background, so that the reflectance of one of the halftones was noticeably impacted by the halo effect and the other one much less impacted. We could rather successfully adjust the period of line halftones to obtain the desired results, both in terms of darkening with the QR-code picture, and in terms of hue, with the Elephant picture. Adjusting the period allowed to act both on the halo effect, which depends on the *d/p* ratio, and on the dot gain effect due to light scattering within the substrate, which tends to impact more halftones having a small period. This could be used towards anti-counterfeiting applications in the future.

References

[1] Neugebauer H.E.J., 'Die Theoretischen Grundlagen des Mehrfarbenbuchdrucks', *Zeitschrift fur Wissenschaftliche Photographie. Photophysik und Photochemie*, vol. 36, no. 4, pp. 73–89, 1937.

[2] A. Murray, 'Monochrome reproduction in photoengraving', *Journal of the Franklin Institute*, vol. 221, no. 6, pp. 721–744, Jun. 1936, doi: 10.1016/S0016-0032(36)90524-0.

[3] D. Wyble and A. Kraushaar, 'The theoretical basis of multicolor letterpress printing, Hans E. J. Neugebauer', *Color Research & Application*, vol. 30, no. 5, pp. 322–331, 2005, doi: 10.1002/col.20135.

[4] F. R. Clapper and J. a. C. Yule, 'The Effect of Multiple Internal Reflections on the Densities of Half-tone Prints on Paper', *J. Opt. Soc. Am., JOSA*, vol. 43, no. 7, pp. 600–603, Jul. 1953, doi: 10.1364/JOSA.43.000600.

[5] J. A. C. Yule and W. J. Nielsen, 'The penetration of light into paper and its effect on halftone reproduction', *Proc. TAGA*, vol. 3, pp. 65–76, 1951.

[6] J.A. Stephen Viggiano, 'Modeling the Color of Multi-Colored Halftones', *TAGA Proceedings*, pp. 44–62, 1990.

[7] F. P. Callahan, 'Light Scattering in Halftone Prints', *J. Opt. Soc. Am., JOSA*, vol. 42, no. 2, pp. 104–105, Feb. 1952, doi: 10.1364/JOSA.42.000104.

[8] F. R. Ruckdeschel and O. G. Hauser, 'Yule-Nielsen effect in printing: a physical analysis', *Appl. Opt., AO*, vol. 17, no. 21, pp. 3376–3383, Nov. 1978, doi: 10.1364/AO.17.003376.

[9] G. Rogers, 'Optical dot gain in a halftone print', *Journal of Imaging Science and Technology*, vol. 41, no. 6, pp. 643–656, Nov. 1997.

[10] D. Modrić, K. P. Maretić, and A. Hladnik, 'Determination of point-spread function of paper substrate based on light-scattering simulation', *Appl. Opt., AO*, vol. 53, no. 33, pp. 7854–7862, Nov. 2014, doi: 10.1364/AO.53.007854.

[11] L. Vallat-Evrard, 'Mesure,analyse et modélisation à l'échelle microscopique de points imprimés pour améliorer les solutions de lutte anti-contrefaçon', Communauté Université Grenoble Alpes, LGP2, 2019.

[12] P. G. Engeldrum and B. Pridham, 'Application of Turbid Medium Theory to Paper Spread Function Measurements', vol. 1, p. 14, 1995.

[13] S. Inoue, N. Tsumura, and Y. Miyake, 'Measuring MTF of Paper by Sinusoidal Test Pattern Projection', *Journal of Imaging Science and Technology*, vol. 41, no. 6, pp. 657–661, Nov. 1997.

[14] F. Dailliez, M. Hébert, L. Chagas, T. Fournel, and A. Blayo, 'Use of Multispectral Microscopy in the Prediction of Coated Halftone Reflectance', *Journal of Imaging*, vol. 8, no. 9, Art. no. 9, Sep. 2022, doi: 10.3390/jimaging8090243.

[15] A. Cornu, 'Sur le halo des lames épaisses, ou halo photographique, et les moyens de le faire disparaitre', *J. Phys. Theor. Appl.*, vol. 9, no. 1, pp. 270–277, 1890.

[16] L. Simonot, M. Hébert, M. Gerardin, C. Monpeurt, and T. Fournel, 'Halo and subsurface scattering in the transparent coating on top of a diffusing material', *Journal of the Optical Society of America A*, vol. 35, no. 7, pp. 1192–12, Jun. 2018, doi: 10.1364/JOSAA.35.001192.

[17] M. Hébert, F. Dailliez, and L. Simonot, 'Why a clear coating modifies halftone color prints', presented at the Material Appearance, IS&T Electronic Imaging Symposium, Online, Jan. 2021.

[18] F. C. Williams and F. R. Clapper, 'Multiple Internal Reflections in Photographic Color Prints', *Journal of the Optical Society of America*, vol. 43, pp. 595–599, 1953.

[19] J. D. Shore and J. P. Spoonhower, 'Reflection Density in Photographic Color Prints: Generalizations of the Williams–Clapper Transform', *Journal of Imaging Science and Technology*, vol. 45, no. 5, pp. 484–488, 2001.

[20] M. Hébert, *Optical Models for Material Appearance*. EDP sciences, 2022. doi: 10.1051/978-2-7598-2647-6.

[21] G. Sharma, W. Wu, and E. N. Dalal, 'The CIEDE2000 color-difference formula: Implementation notes, supplementary test data, and mathematical observations', *Color Research & Application*, vol. 30, no. 1, pp. 21–30, 2005, doi: 10.1002/col.20070.

Author Biography

Fanny Dailliez graduated from the University Jean Monnet and from the Institut d'Optique Graduate School in 2020. She is now a PhD student at the LGP2 of Université Grenoble Alpes and at the Laboratoire Hubert Curien of University Jean Monnet of Saint-Etienne in France. Her thesis project deals with the appearance of printed artifacts to improve anticounterfeiting strategies.